0888-8809/02/$15.00/0
Printed in U.S.A.

Molecular Endocrinology 16(4):722–735

Lysine 183 and Glutamic Acid 157 of the TSH Receptor: Two Interacting Residues with a Key Role in Determining Specificity toward TSH and Human CG

GUILLAUME SMITS, CÉDRIC GOVAERTS, ISABELLE NUBOURGH, LEONARDO PARDO, GILBERT VASSART, AND SABINE COSTAGLIOLA

Service de Génétique Médicale (G.S., G.V.), Hôpital Erasme, B-1070 Bruxelles, Belgium; Institut de Recherche Interdisciplinaire en Biologie Humaine et Nucléaire (G.S., C.G., I.N., G.V., S.C.), Université Libre de Bruxelles, Campus Erasme, B-1070 Bruxelles, Belgium; Service de Conformation des Macromolécules Biologiques (C.G.), Université Libre de Bruxelles, 1050 Bruxelles, Belgium; Laboratori de Medicina Computacional (L.P.), Unitat de Bioestadística, Facultat de Medicina, Universitat Autònoma de Barcelona, 08193 Bellaterra, Spain

A naturally occuring mutation in the ectodomain of the TSH receptor (TSHr), K183R, has been described recently in a familial case of gestational hyperthyroidism. Hyperthyroidism was explained by the widening of the specificity of the mutant receptor toward human CG (hCG). In the present study, we attempted to understand in molecular terms the structure-phenotype relationships of this mutant in light of the available structural model of TSHr ectodomain established on the template of the atomic structure of the porcine ribonuclease inhibitor. To this aim, we studied by site-directed mutagenesis and functional assays in transfected COS cells the effects of substituting amino acids with different physicochemical properties for lysine 183. Unexpectedly, all TSHr mutants displayed widening of their specificity toward hCG. Molecular dynamics simulations suggested that the gain of function would be secondary to the release of a nearby glutamate residue (E157) from a salt bridge with K183. This hypothesis was supported by further site-directed mutagenesis experiments showing that the presence of an acidic residue in position 157, or in its vicinity, was required to observe the increase in sensitivity to hCG (an acidic residue in position 183 can partially fulfill the role of a free acidic residue in position 157 when tested on the background of a E157A mutant). Our results suggest also that additional natural mutations (especially K183M, N, or Q) in position 183 of TSHr are expected to be found in gestational hyperthyroidism. (*Molecular Endocrinology* 16: 722–735, 2002)

THE TSH RECEPTOR [TSHr (1, 2)], a rhodopsin-like G protein-coupled receptor, constitutes with the lutropin/CG (3–5) and the follitropin receptors [LH/CGr, and FSHr, respectively (6)] the glycoprotein hormone receptor family. The corresponding hormones, TSH, LH, or human CG (hCG) and FSH, are dimers made of a common α-subunit and receptor-specific β-subunits (7, 8). Despite sequence similarity, both between the individual receptors and the β-subunits of the hormones, each ligand-receptor couple plays a distinctive role in thyroid (TSH $\leftrightarrow$ TSHr) and reproductive physiology (FSH $\leftrightarrow$ FSHr, LH/CG $\leftrightarrow$ LH/CGr) thanks to the tight binding specificity they display (9–13).

The glycoprotein hormone receptors exhibit a bipartite structure with a clear functional dichotomy: the amino-terminal half constitutes an ectodomain responsible for high affinity binding of the hormones (14–18); the carboxyl-terminal portion with a rhodopsin-like serpentine structure containing seven transmembrane α-helices is responsible for transduction of the signal, mainly to Gs (see Fig. 1A; Refs. 19–21). The ectodomain contains a central portion of nine leucine-rich repeats (LRR) bordered by two cysteine-rich domains, typical of the large family of LRR proteins (22). Structural models of the extracellular part of the glycoprotein hormone receptors based on the atomic structure of the porcine ribonuclease inhibitor (23) have been proposed (24–26). According to these models, each LRR comprises 20–24 amino acids forming a β-strand followed by an α-helix. The LRR units are arranged with their β-strands and α-helices parallel to a common axis and organized spatially to form a horseshoe-shaped molecule with the β-strands and α-helices making the concave and convex surfaces of the horseshoe, respectively (Fig. 1B). By analogy with the atomic structure of the ribonuclease-ribonuclease inhibitor complex (23), it is assumed that hormones make contact, mainly but not exclusively, with the β-sheets of the inner concave portion of the horseshoe.

A typical β-strand of a LRR is composed of 8 amino acids $LX_1X_2LX_3LX_4X_5$ (where X is any amino acid, and

Abbreviations: 3D, Three-dimensional; EC_{50}, 50% effective concentration; FSHr, FSH receptor; hCG, human CG; LH/CGr, LH and CG receptor; LRR, leucine-rich repeat; ps, picosecond; TSHr, TSH receptor; wt, wild type.

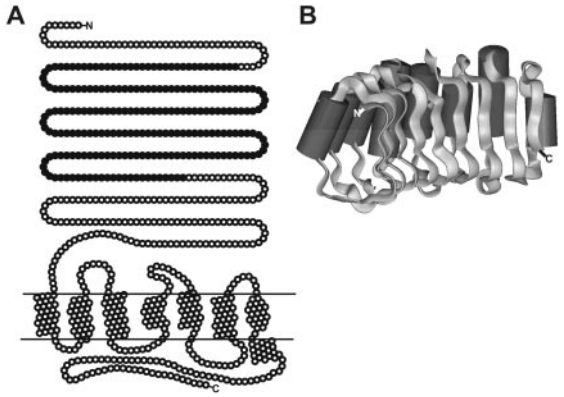

Fig. 1. Schematic Representation of the TSHr (A) and Ribbon Representation of the Model of the LRR Region (B)

A, The seven-transmembrane helices are drawn as helical nets, respecting the helice ends as observed in the crystal structure of rhodopsin (21); the cytoplasmic helix (helix 8) is also represented. *Closed circles* in the N-terminal extension represent the portion of the domain modeled by Kajava *et al.* (24), comprising residues 54–254. B, The α-helices are drawn as *solid tubes*. The "horseshoe" curvature is clearly visible.

L is leucine, isoleucine, valine, or, rarely, methionine or alanine; Ref. 24). According to the proposed structural models (24–26), the side chains of L amino acids are pointing inside the hydrophobic core of the protein, whereas those of the X residues are directed toward the surface of the protein. Exposed side chains on the inner face of the horseshoe are supposed to contact the ligands (24–26). This is supported by the observation that they are mostly not conserved between the three glycoprotein hormone receptors, which, in turn, suggests that they could be responsible for the binding specificity.

In 1998, we described a familial case of gestational hyperthyroidism caused by a mutation of one of these exposed residues in the ectodomain of the TSHr (27). The mutation substituted an arginine for the lysine in position 183, with the result that the mutant displayed widening of its specificity toward hCG. Because of the very high plasma concentrations of hCG during pregnancy, the patients suffered from severe hyperthyroidism, requiring treatment with antithyroid drugs throughout pregnancy. In the present study, we attempted to understand in molecular terms the structure-phenotype relationships of this mutant in light of the structural model described above. To this aim, we studied by site-directed mutagenesis and functional assays in transfected COS cells the effects of substituting amino acids with different physicochemical properties for lysine 183. The results indicated unexpectedly that the gain of function toward hCG displayed by the K183R mutant could be mimicked by all different amino acid substitutions tested in this position. Molecular dynamics simulations suggested that the gain of function might be secondary to the release of a nearby glutamate residue (E157) from a salt bridge with K183. This hypothesis was supported by further site-directed mutagenesis experiments showing that the presence of an acidic residue in position 157, or in its vicinity, was required to observe the increase in sensitivity to hCG.

RESULTS

Any Change at Position 183 of the TSHr Increases Its Sensitivity to hCG

To determine whether the gain of function caused by the K183R mutation in the patient with gestational hyperthyroidism was the direct consequence of the presence of an arginine in position 183 of the ectodomain of the TSHr, a series of mutants were engineered in which lysine 183 was replaced by amino acids with different physicochemical properties. Individual mutants were tested by transient expression in COS cells followed by intracellular cAMP determination after stimulation by hCG. All mutants tested were expressed at the cell surface [ranging from 21% to 100% of wild-type (wt) expression], as assayed by flow immunocytometry using the monoclonal antibody 3G4 (Fig. 2A; see *Materials and Methods*). Quite unexpectedly, each mutant displayed increased responsiveness to hCG, with the 50% effective concentration [EC_{50}] (ranging from 7 to 58 IU/ml hCG) grossly similar to that of the K183R mutant (27 $\pm$ 3 IU/ml hCG; Fig. 2, B and C, and Table 1). The wt receptor showed a very small response (Fig. 2, B and C). Considering the widely different physicochemical characteristics of the amino acids substituted for the wt residue in position 183, these results indicated that the gain of function was most probably related to the loss of the lysine rather than to the presence of the substitute.

Apart from their gain of sensitivity to hCG, some of the mutants displayed alteration of their basal ability to stimulate adenylyl cyclase (Fig. 2, B and C). When it is normalized to the level of expression of the mutants at the cell surface, this effect is of minimal amplitude (0.5- to 2-fold, data not shown). Specially designed experiments would be needed to evaluate its potential functional significance.

Modeling the Effects of Mutations at Position 183

The atomic model of the portion of TSHr ectodomain made of LRRs (from residue 54 to 254) built by Kajava *et al.* (24) on the template of the porcine ribonuclease inhibitor provides a structural framework to understand the possible effect of the mutations. Unrestrained molecular dynamics simulations of the TSHr ectodomain in water (see *Materials and Methods*) have been used to model the interactions between the side chains of the ectodomain, focusing on K183 and its surroundings. The results of these computer simulations suggest that K183 is implicated in a direct interaction with its neighbor residue, E157. As illustrated on the representative structure shown in Fig. 3 (*first row,*

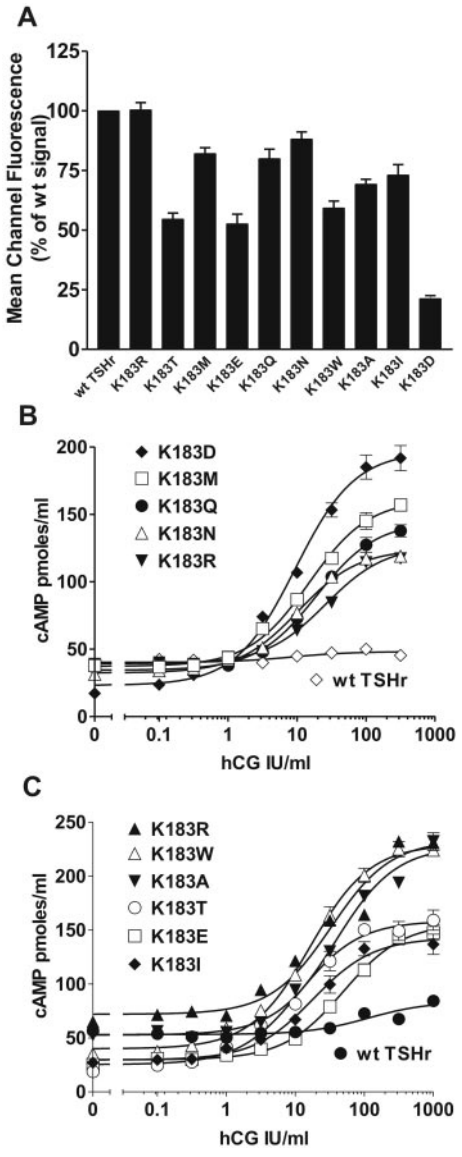

Fig. 2. Functional Assays of K183 Mutant TSHr Constructs after Transfection in COS-7 Cells: Sensitivity to hCG

A, Cell surface expression of K183-substituted mutants. Quantification of cell surface expression was realized by flow cytofluorometry (see *Materials and Methods*). Results are expressed as the percentage of the value obtained in the same experiment for the wt TSHr. B and C, Concentration-action curves for K183-substituted mutants under stimulation by increasing concentrations of hCG. COS-7 cells transiently transfected with the various constructs were stimulated by increasing concentrations of hCG, and intracellular cAMP values were determined by RIA. Results are expressed as picomoles cAMP per milliliter. The Prism computer program (GraphPad Software, Inc.) was used for curve fitting and for EC_{50} calculation. Each *curve* is representative of at least two separate experiments. The variable levels of cAMP observed for the various constructs in the absence of any stimulation by hCG are related to their constitutive activity and to their different level of expression. For the mean EC_{50} values, see Table 1.

Table 1. Mean EC_{50} Values Obtained for hCG and TSH Stimulation of wt and Mutant TSHr

Transfected TSHr constructs	EC_{50} ± range (hCG IU/ml)	EC_{50} ± range (TSH mIU/ml)
wt	>1000	0.060 ± 0.013
K183R	27 ± 3[a]	0.051 ± 0.002
K183A	30 ± 9	0.067 ± 0.003
K183I	16 ± 3	0.064 ± 0.013
K183T	9 ± 2	0.049 ± 0.014
K183E	58 ± 8	0.104 ± 0.042
K183W	14 ± 2	0.051 ± 0.002
K183D	7 ± 1[a]	0.037 ± 0.007
K183M	13 ± 1[a]	ND
K183N	12 ± 1[a]	ND
K183Q	18 ± 3[a]	ND
E157A	>1000	0.295
E157A + K183R	>1000	0.581 ± 0.155
E157A + K183A	>1000	0.275 ± 0.107
E157A + K183I	>1000	0.543 ± 0.032
E157A + K183T	>1000	0.277 ± 0.190
E157A + K183E	58 ± 10[a,b]	0.047 ± 0.010
E157A + K183W	>1000	0.179 ± 0.023
E157A + K183D	16 ± 2	0.088 ± 0.022
E157D	48 ± 14[c]	ND
E157D + K183R	13 ± 7	ND
E157D + K183A	26 ± 6	ND
E157D + K183W	20 ± 6	ND

COS-7 cells were transiently transfected with the following constructs: wt TSHr, K183R, A, I, T, E, W, D, M, N or Q, E157A or D, E157A + K183R, A, I, T, E, W, D, M, N or Q, and E157D + K183R, A or W. Transfected COS-7 cells were stimulated by increasing concentrations of hCG or TSH, and intracellular cAMP values were determined by RIA. Prism computer program (GraphPad Software, Inc.) was used for curve fitting and for EC_{50} calculation. Each concentration-action curve has been realized at least twice (except E157A). The EC_{50} values presented are the arithmetic mean of the two EC_{50} values experimentally obtained. The range of the duplicate determinations is indicated. [a], Arithmetic mean of three EC_{50} values ± SEM. [b], Low amplitude of stimulation (see Fig. 4D). [c], Very low amplitude of stimulation (see Fig. 5B). ND, Not done.

left panel), the side chain of K183 is nicely positioned to achieve a salt bridge with one of the carboxyls of glutamate 157 (observed in 80% of the structures from the production phase of the simulation). E157 is also found to interact with another basic residue, R109 (observed in 100% of the structures). Further analysis of the model shows that the numerous charged or polar residues exposed in the surroundings of K183 (the inside of the horseshoe) are predicted to form a large and complex network of polar interactions. Therefore, we computed the electrostatic potential at the accessible surface of the model, using the program GRASP, to visualize the effects of these interactions on the overall distribution of charges (see *Materials and Methods*). As shown in Fig. 3 (*first row, right panel*), the electrostatic distribution is clearly asymmetrical. The N-terminal part of the horseshoe (the *left side of the picture*) appears positively charged (*col-*

ored in blue), due to the presence of K58, R80, R109, and K183, which completely shield the acidic residues E107 and E157. On the *right side of the picture*, the C-terminal part is on average negatively charged (*colored in red*), mainly due to the presence of D203, D232, and E251 [R255 is not included in the model of Kajava *et al.* (24)].

Using the same starting structure but changing the side chain of residue 183, we modeled similarly the possible side-chain interactions in the context of the K183A mutant. As expected, E157 now only interacts with R109, resulting in a modification of the organization of the polar network (Fig. 3, *second row, left panel*). This is clearly visible from the electrostatic surface potential (Fig. 3, *second row, right panel*), which shows a strong modification of the electrostatic equilibrium. The N-terminal side (*left*) appears now less positively charged than in the wt, with K58 protruding as the only positive charge and the other basic residues being balanced by acidic partners. Quite clearly, the negative area has now extended up to E157, resulting in an accessible surface that is significantly more negative than what we observed for the wt simulation.

In summary, in the wt receptor, E157 appears to be shielded by positively charged residues, namely R109 and K183. Mutations of K183 into alanine modifies strongly the electrostatic pattern, inducing an increase in negatively charged areas, in particular around position 157. Similar structural effects would be expected to result from substitutions of K183 by any non-basic amino acid, providing a satisfactory explanation for the phenotypes observed for the mutations of K183 into A, I, T, E, D, M, N, Q, or W. The increase of stimulation by hCG in the case of the conservative K183R mutation would require a different explanation, implying that the R183 mutant would achieve a different spatial organization of its electrostatic potential, when compared with the wt structure (see below and *Discussion*).

E157 Is Implicated in the Stimulation of TSHr K183 Mutants by hCG

To test the hypothesis that the increased responsiveness of the mutants to hCG was due to the release of E157 from a neutralizing interaction with K183, we created a series of double mutants in which, in addition to the substitutions in position 183 (K183R, A, I, T, E, W, M, N, or Q), an alanine was substituted for glutamic acid in position 157. The E157A mutation was also introduced in the wt TSHr as a control. All the double mutants and E157A were well expressed at the surface of transfected COS-7 cells (expression ranging from 47 to 83% of wt, Fig. 4A). When stimulated by high concentrations of hCG, none of the mutants displayed increase in cAMP production with the exception of the E157A+K183E mutant (Fig. 4, B and C). This indicates an important role of E157 in the interaction with hCG, supporting the hypothesis of an indirect role for mutations at position 183. Notably, the E157A+K183E mutant responded to hCG with an EC_{50} (58 $\pm$ 10 IU/ml) in the same range as that of K183 single mutants (ranging from 7 to 58 IU/ml hCG, Fig. 4D). A likely interpretation for the exceptional phenotype of this particular construct amongst the double mutants is that a glutamic acid in position 183 would somehow fulfill the role achieved by E157 in the single mutants (*e.g.* K183A). Molecular modeling of the E157A+K183E double mutant further supports this hypothesis. As shown in Fig. 3 (*third row*), mutating both E157A and K183E produces a model whose electrostatic surface potential is quite similar to that of the single K183A mutant. The *left side* of the model is overall positively charged, as observed for the wt and the K183A mutant, whereas the *right side* is negatively charged. The presence of E183 induced an extension of the negatively charged area up to the middle of the structure, making it quite similar to the K183A model. It is tempting to propose that the increased sensitivity to hCG observed in the E157A+K183E double mutant is due to the same mechanism as for most K183 single mutants (*i.e.* increase in negative potential around positions 157 or 183).

There may be a slight inverse agonistic effect of hCG on E157A and some E157A double mutants (Fig. 4B). This effect, which might alternatively correspond to toxicity of high hCG concentrations, could be interesting to explore in the future. In addition, some of the mutants displayed alteration of their basal ability to stimulate adenylyl cyclase (Fig. 4, B–D). As already mentioned for K183 single mutants, when it is normalized to the level of expression of the mutants at the cell surface, this effect is of minimal amplitude (0.7- to 2.5-fold, data not shown).

Gain of Responsiveness to hCG Is Dependent on the Presence of a Negative Charge in Position 157 or 183

Aspartic acid was substituted for glutamic acid in position 157 in the wt TSHr, the K183R, K183A, and K183W mutants. All mutants were expressed at the surface of COS cells, although the E157D+K183A and the E157D+K183W mutants displayed low expression [54, 86, 13, and 10% of wt for E157D, E157D+K183R, E157D+K183A, and E157D+K183W, respectively (Fig. 5A)]. In agreement with the hypothesis, all three double mutants displayed increased response to hCG, as compared with the E157D single mutant (Fig. 5B). Note, however, that the E157D single mutant shows also a very small response to hCG allowing determination of an EC_{50} value (48 $\pm$ 14 IU/ml). It is conceivable that the shorter side chain of an Asp in position 157 would be less efficiently neutralized by K183, thus allowing it to interact with hCG.

Most interestingly, the E157A+K183D double mutant [which is expressed at the surface of COS cells at 48% of wt (Fig. 5A)] could also be stimulated by hCG (EC_{50} = 16 $\pm$ 2 IU/ml; Fig. 5C), demonstrating

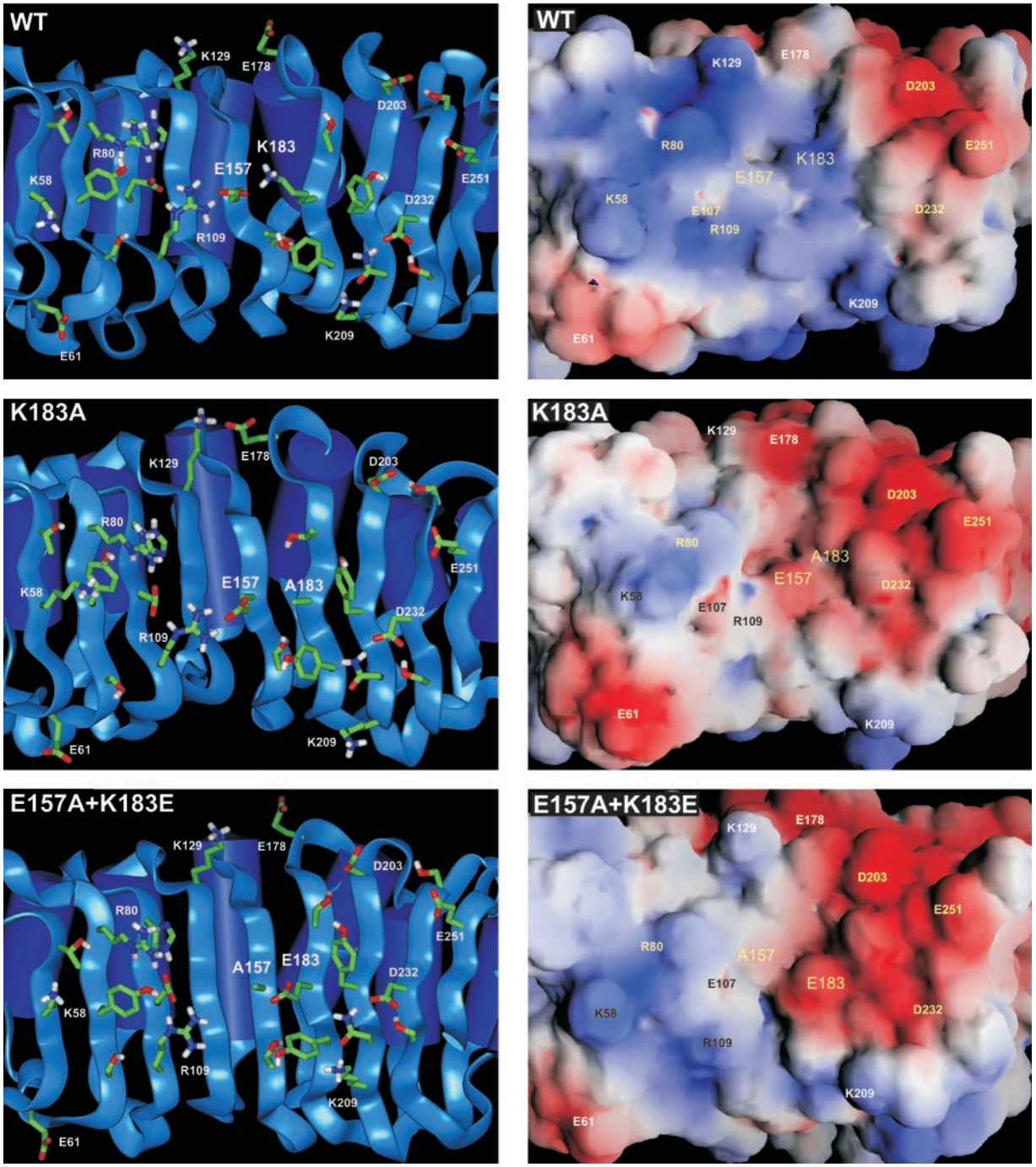

Fig. 3. Representative Models of the Molecular Dynamics Simulations

For the wt TSHr and the K183A and E157A+K183E mutants, representative structures from the molecular dynamics simulations (see *Materials and Methods*) are depicted. On the *left side*, the models are represented as *ribbons*, with the α-helices as *tubes*. Charged and polar side chains facing the interior of the horseshoe are explicitly shown as *solid sticks*, with the polar hydrogen atoms in *white*, carbons in *green*, nitrogen atoms in *blue*, and oxygen atoms in *red*. The side chains of residues E61, K129, E178, D203, and K209 are also shown to provide a complete view of the charged amino acids possibly important for the electrostatic landscape. On the *right side*, electrostatic potential maps of the corresponding structures are shown. The maps were built with the GRASP software (see *Materials and Methods*), with the color scale for charges going from -4 (*red*) to $+4$ (*blue*). The positions of the charged side chains are indicated.

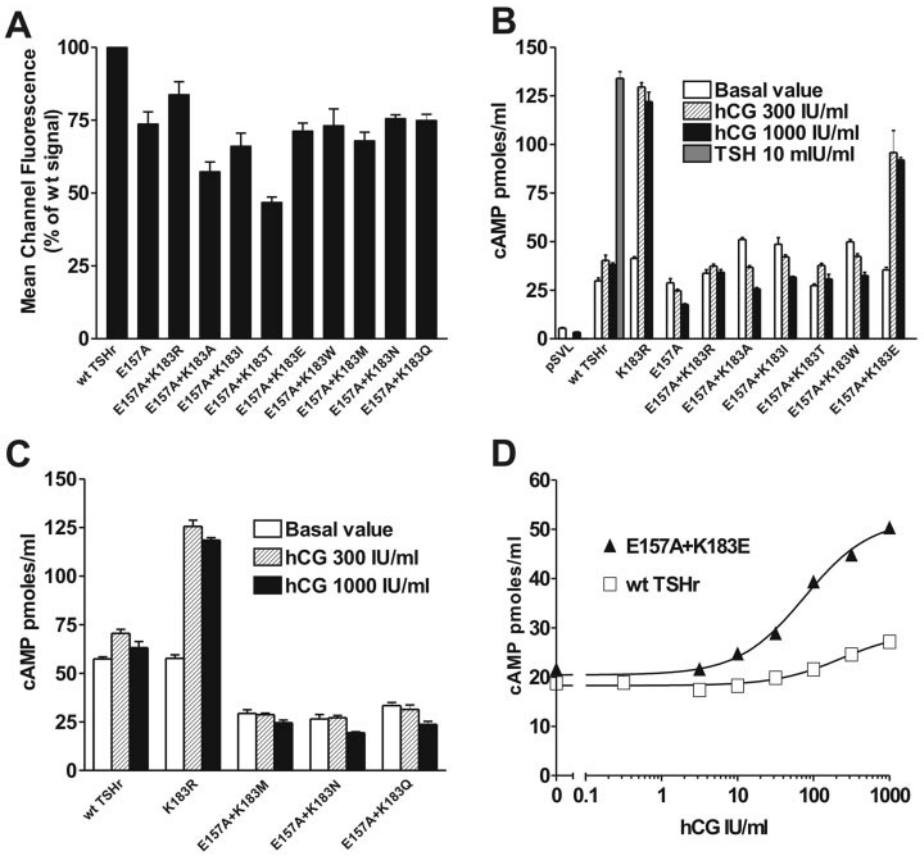

Fig. 4. Functional Assays of E157A and E157A+K183X Mutant TSHr Constructs after Transfection in COS-7 Cells: Sensitivity to hCG

The following constructs have been investigated: wt TSHr, E157A, and E157A+K183R, A, I, T, E, W, M, N, or Q mutants. A, Quantification of cell surface expression was realized by flow cytofluorometry as described in the legend to Fig. 2. B and C, Stimulation of cAMP accumulation in COS-7 cells transfected with wt TSHr, E157A, and E157A+K183X constructs after stimulation by high concentrations of hCG. Each *point* represents the mean cAMP value of at least two replicates. D, Concentration-action curve for the E157A+K183E mutant construct and the wt TSHr under stimulation by hCG. Results of cAMP accumulation in transiently transfected COS-7 cells are expressed and fitted as described in the legend to Fig. 2. The *curve* is representative of three separate experiments. For the mean EC_{50} value, see Table 1.

that the gain of responsiveness to hCG was dependent on the presence of a negative charge in position 157 or 183.

Modeling the Effects of the K183R Mutant

The above experimental results suggest that Arg, when present at position 183, interacts with a different partner than E157. In the three-dimensional (3D) model used here, three others acidic residues appear to be accessible to R183, namely D160, D203, and D232. The interatomic distances between the α-carbon positions of R183 and D160, D203, or D232 residues are compatible with such an interaction (9.5, 11.2, and 9.3 Å, respectively). The longer side chain of arginine compared with lysine might facilitate the interaction with these more distant residues. To identify the potential ionic partners of R183, we surveyed all possible conformations of the Arg side chain using a backbone-dependent rotamer library (Ref. 28; see *Materials and Methods* for computational details). The E157↔R183 interaction is favored in 8 different conformations of the 81 conformations theoretically accessible to an Arg side chain. These 8 rotamers were observed in 31% of the crystal structures in the original protein-structure survey statistics (28). The R183↔D232 interaction was favored by 6 allowed rotamers (amounting to 8% of the observed conformations in the survey), whereas the R183↔D160 interaction was allowed in only 1 case (5%), and the R183↔D203 interaction was never favored by any of the allowed rotamers. We modeled the three possible interactions using the most probable rotamer in each case; *i.e.* the g+,t,t,t conformation, the t,t,t,g+ conformation and the g+,g+,t,t conformation for the E157↔R183, D160↔R183 and R183↔D232 interactions, respectively. The molecular modeling procedure revealed that direct interaction with D160 required the Arg side chain to extend between the β-strands of the LRR_5

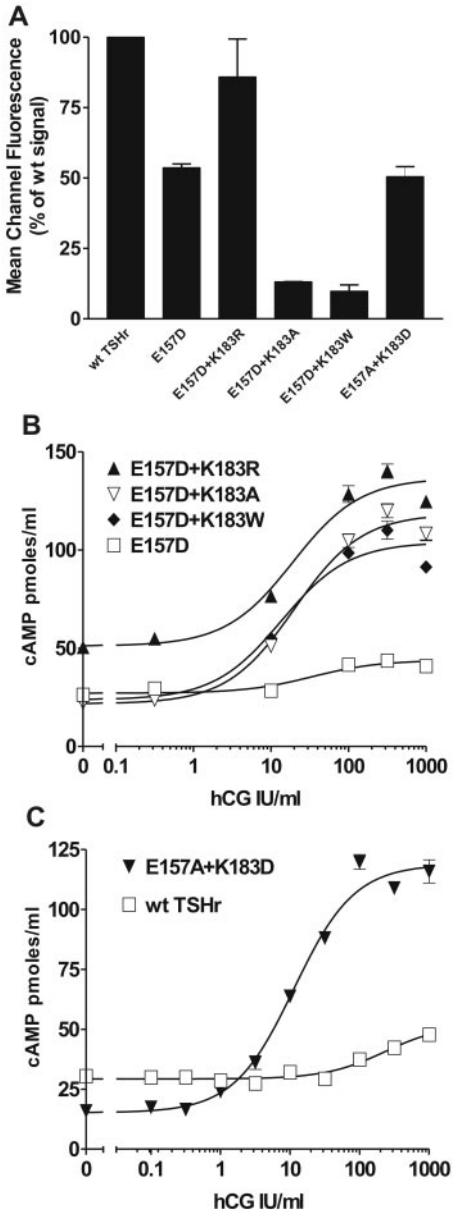

Fig. 5. Functional Assays of E157D, E157D+K183X, and E157A+K183D Mutant TSHr Constructs after Transfection in COS-7 Cells: Sensitivity to hCG

The following constructs have been investigated: wt TSHr, E157D, E157D+K183R, A or W, and E157A+K183D mutants. A, Quantification of cell surface expression was realized by flow cytofluorometry as described in the legend to Fig. 2. B and C, Concentration-action curves for the E157D, E157D+K183R, A or W, and E157A+K183D mutant constructs under stimulation by hCG. Results of intracellular cAMP accumulation in transiently transfected COS-7 cells are expressed and fitted as described in the legend to Fig. 2. Each *curve* is representative of two separate experiments. For the mean EC_{50} values, see Table 1.

and LRR_6. The steric clash of R183 with the β-branched side chain of T159 and the side chain of Y185 contributing to LRR_5 and LRR_6 prevents this contact (not shown here). Thus, in addition to E157, D232 appears the most likely partner for R183.

Figure 6A shows a representative structure of the unrestrained molecular dynamics simulation of the K183R mutant forming an ionic bridge with E157. Importantly, in contrast to the ammonium group of lysine, the guanidium group of arginine can form multiple interactions via its N_ϵ, N_{H1}, and N_{H2} moieties. Thus, the single free O_δ atom of E157 (the other O_δ atom interacting with R109; see Fig. 3) interacts with the N_ϵ moiety of R183 (observed in 70% of the structures from the production phase of the simulation), whereas the other N groups are exposed to the solvent and interact only with water molecules (not shown). As shown in Fig. 6B, the ionic interaction of R183 with E157 yields a model whose electrostatic surface potential is similar to that of the wt model (Fig. 3, *first row, right panel*), with the positively charged region (*blue area*) extending beyond the center of the horseshoe. In summary, in the case of a E157↔R183 interaction, the K183R mutant would behave electrostatically in a similar way as the wt model and R183 would be strongly solvated.

The interaction of R183 with D232 involves a more complex network of hydrogen bonds between the guanidium group of Arg and the nearby residues Y185, Y206, and N208 (see Fig. 6C). In addition to the direct interaction with one of the carboxyl O_δ atoms of D232, R183 also forms hydrogen bonds with the O_δ atom of N208, and the π electrons clouds of Y185 and Y206. This type of N-H··π interaction is known to play a significant role in stabilizing local 3D structures of proteins (29). To evaluate the magnitude of this N-H··π interaction, we performed *ab initio* quantum mechanical calculations on minimal recognition models consisting of the functional groups of the intervening side chains (see *Materials and Methods*). This allowed us to evaluate energy terms that are not well represented in molecular mechanics calculations (*i.e.* N-H··aromatic interactions and resonant H-bond networks). Interestingly, the system, fully optimized with no constraints, adopts relative orientation of the side chains resembling the model obtained in the molecular dynamics simulation (see Fig. 6, C and E). The energy of interaction between Y185 and Y206 with the R183/N208/D232 fragment is −11.2 and −9.2 kcal/mol, respectively. Accordingly, there is a significant contribution of the aromatic side chains of Y185 and Y206 in the stabilization of a rotamer conformation of R183 that allows interaction with D232. However, it is important to note that during the unrestrained molecular dynamics simulation, this complex hydrogen bond network was not preserved until the end. The side chain of R183 ultimately reoriented toward the solvent. We attribute this behavior to the underestimation of N-H··aromatic interactions, compared with N-H··water interactions, in molecular mechanics force fields.

Figure 6D shows the electrostatic potential of the model displayed in Fig. 6C, in which R183 interacts with D232 and neighboring residues. The conforma-

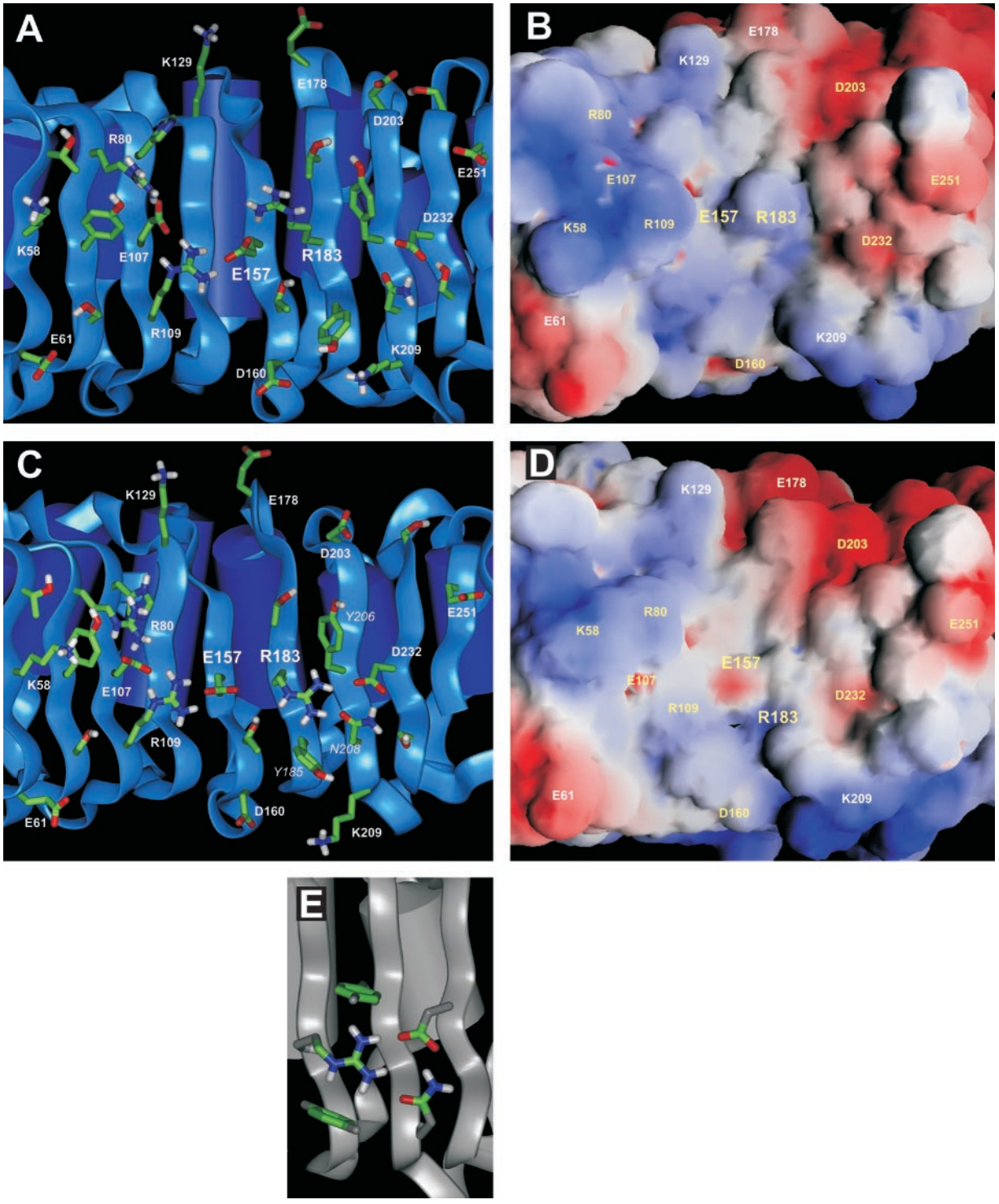

Fig. 6. Conformational Study of the K183R Mutant

A, Representative structure of the K183R mutant model from the molecular dynamics simulations (see *Materials and Methods*) favoring the E157↔R183 interaction. Rendering is similar to that in Fig. 3. B, Electrostatic potential map of the model depicted in A; parameters were chosen as in Fig. 3. C, Model of the K183R mutant favoring the R183↔D232 interaction. D, Electrostatic potential maps of the model depicted in C. E, Optimal conformation of the proposed interacting motif obtained by *ab initio* quantum mechanical calculations (see *Materials and Methods* and text for details). The actual motif used for calculations is depicted in *color* (*green* for carbon, *blue* for nitrogen, *red* for oxygen, and *white* for hydrogen atoms). Extension of the side chains and ribbon representation of the model are shown in *gray* for illustration purposes, allowing to observe the similarity with the motif represented in C.

tion of R183 significantly influences the electrostatic map at the molecular surface. Despite the fact that the net charge of the system remains the same, the positively charged area around position 157 becomes much smaller if, instead of interacting with E157, R183 interacts with D232 (compare Fig. 6, B and D). E157 becomes accessible, inducing a negatively charged region in the center of the model. Hence, this conformation leads to an electrostatic potential map resembling that of the K183A model (Fig. 3, *second row, right panel*), providing a structural rationale to the similar of phenotype of the two mutants.

In summary, although both negative partners (E157 and D232) are geometrically accessible to R183, the R183↔D232 conformation would be favored by the additional stabilizing interactions (*i.e.* N-H··π). This conformation displays little solvation of R183 and is electrostatically close to the other K183 mutants. In the case of the wt receptor, a K183↔D232 is unlikely because 1) this interaction can happen in only one allowed rotamer, representing 1% of all observed conformations (using similar criteria as for K183R) due to the shorter side chain of lysine, and 2) stabilizing interaction with surrounding side chains would not take place as a lysine has only one active group (the ammonium moiety involved in the salt bridge). K183 would therefore preferentially interact with the closer E157.

Gain of Function of K183 Mutants Is Specific for hCG

Finally, we explored whether the gain of function displayed by K183 mutants was restricted to stimulation by hCG or could also be observed for TSH or FSH. Some of the mutants (K183R, A, I, T, E, W, or D; E157A; E157A+K183R, A, I, T, E, W, or D) were challenged with TSH and the EC_{50} values were determined. As illustrated in Fig. 7 and Table 1, all mutants were readily stimulated by TSH; for the single mutants, their EC_{50} values were in the same range (0.037–0.104 mIU/ml) as for the wt receptor (0.060 ± 0.013 mIU/ml); for the double mutants, EC_{50} values were generally higher (0.179–0.581 mIU/ml) except for E157A+K183E and E157A+K183D, which displayed a wt value (0.047 ± 0.010 and 0.088 ± 0.022 mIU/ml, respectively). Similarly, the wt TSHr and K183R, A, or W mutants were subjected to stimulation by FSH. No stimulation of cAMP production could be observed at the maximal concentration assayed (30 IU/ml, *i.e.* 10^3 times the EC_{50} for the FSHr; data not shown). From these experiments, we conclude that the overall 3D structure of the mutants is well preserved (as they are all readily

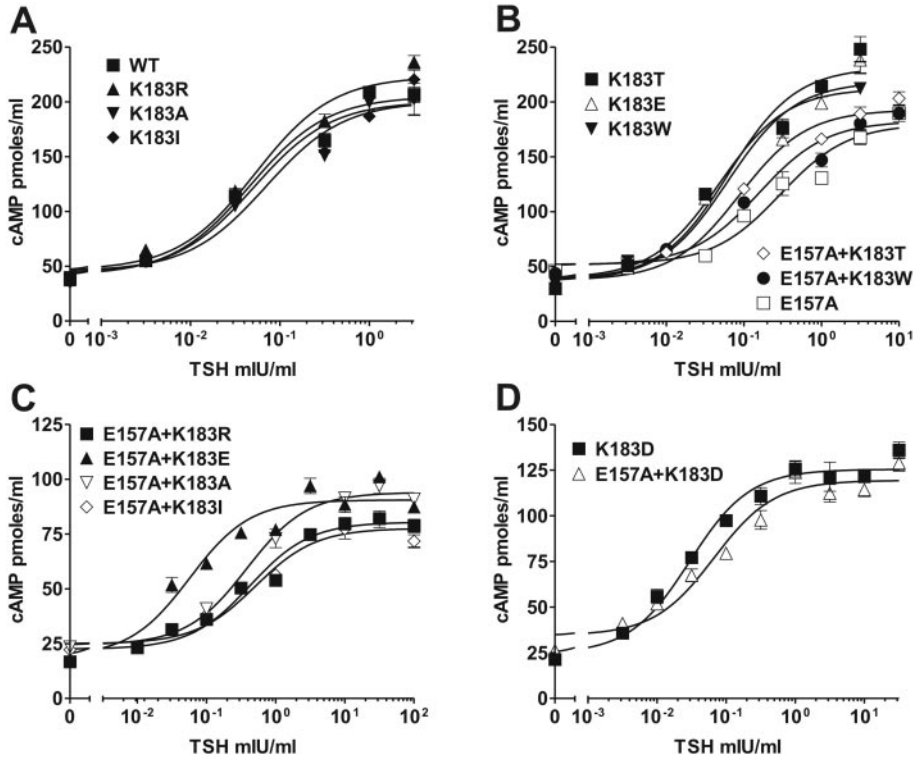

Fig. 7. Functional Assays of K183X and E157A+K183X Mutant TSHr Constructs after Transfection in COS-7 Cells: Sensitivity to TSH

The following constructs have been investigated: wt TSHr, K183R, A, I, T, E, W or D, E157A and E157A+K183R, A, I, T, E, W or D. The results of intracellular cAMP accumulation in transiently transfected COS-7 cells after stimulation by increasing concentrations of TSH are expressed and fitted as described in the legend to Fig. 2. Each *curve* is representative of two separate experiments. For the mean EC_{50} values see Table 1.

stimulated by TSH) and that the gain of function, when present, is specific of hCG.

Gain of Sensitivity of K183 Mutants Does Not Lead to Measurable Binding of hCG

Despite the increase in sensitivity to hCG displayed by a series of TSHr mutants bearing amino acid substitutions in position K183, and by the E157A+K183E double mutant, the affinity of the mutants for hCG was too low to permit detection of specific binding of labeled hCG. Similarly, excess unlabeled hCG was unable to compete for ^{125}I-TSH binding to the mutants (not shown). Considering that the EC_{50} of our mutants for hCG is about 1,000 times higher than that of the wt LHr, this is compatible with binding experiments being less sensitive than stimulation experiments to detect low affinity interactions.

DISCUSSION

The Salt Bridge Hypothesis

The effects of substituting amino acids with different physicochemical properties for the K183 residue of the TSHr indicated that, contrary to our expectation, the gain of function toward hCG displayed by the K183R mutant was due to the loss of the lysine residue rather than to the presence of the arginine.

Molecular dynamics simulations carried out with the model of Kajava *et al.* (24) as a starting point indicated that K183 would be involved in a salt bridge with the nearby E157, suggesting that the gain of function toward hCG of mutants in position 183 would be secondary to the generation of a negatively charged area in this portion of the ectodomain. The observation that in the double mutant series, with E157 mutated to alanine and K183 replaced by various amino acids, only the E157A+K183E and E157A+K183D constructs showed that responsiveness to hCG is a strong argument in favor of this hypothesis. Altogether, our results suggest that hCG mainly needs an accessible acidic residue in position 157 of the ectodomain (or in the nearby 183 position, like in the E157A+K183E and E157A+K183D double mutants) to stimulate the mutant TSH receptors.

Ironically, the mutant described originally, K183R, is the most difficult to fit in the above model. Indeed, one would intuitively assume that both an arginine and a lysine, when present in position 183, would be able to establish a salt bridge with E157. Our experimental results imply that this is not the case, suggesting that, when an arginine is present in 183, it would interact with a different partner than E157. Molecular modeling indicates that the free side chain of D232 is the likely alternative partner for R183. However, available methods do not allow the determination of whether the conformation of R183 pointing toward D232 is more stable than the conformation of R183 pointing toward E157. In both conformations, R183 forms an ionic interaction with a single oxygen atom (of E157 or D232). Notably, the Arg conformation achieving interaction with E157 is stabilized by hydrogen bonds between the other N groups of R183 and surrounding water molecules, whereas the interaction with D232 is additionally stabilized by hydrogen bonds with the side chains of other residues: Y185, Y206, and N208.

The formation of the TSHr-hCG complex is a function, among others parameters, of the interaction energy between the ligand and the receptor, and the energy required to displace, totally or partially, the water molecules from the interacting surface. The observation that the phenotype of the K183R mutant is highly similar to that of the K183A mutant (see Fig. 2C) suggests that R183 does not directly participate in the interaction between the receptor and hCG and that no desolvation of R183 is required for hCG binding. The side chain of R183 interacting with E157 is exposed to the interacting surface (see Fig. 6A) and is heavily solvated. This is at variance with the comparable K183A and K183R phenotypes. In contrast, the side chain of R183 interacting with D232 is hidden to the ligand and is weakly solvated, as every polar moiety is involved in at least one hydrogen bond with other side chains of the receptor (namely Y185, Y20, and N208; see Fig. 6C). Thus, we strongly favor the hypothesis that R183 would interact mostly with D232 and rarely with E157.

It must be stressed that there may be other structural interpretations to our observations. We must be open to the possibility that the horseshoe model of the ectodomain, which is certainly incorrect in its details, might be grossly incorrect altogether. Another way to account for the gain of function of mutants in position 183 is to consider that K183 would be free in wt TSHr and repulsive for hCG. Removal of the lysine would then result in an increase in sensitivity for hCG. This hypothesis would fit the negative determinant theory (12, 30). However, it would face the same difficulty to account for the phenotype of the original K183R mutant, which would be expected to exhibit a similar repulsive behavior. Also, this scenario would not provide an explanation to the phenotypes of the E157A+K183X double mutants. Whatever the final structural explanation for our observations, which will have to wait for crystallographic data, our results establish a definite relationship between the gain of function of K183 mutants and the presence of an acidic amino acid in position 157.

The Homologue Residue to K183 of TSHr Is also a Lysine in LHr

In the LH/CGr, the residue corresponding to K183 is also a lysine (K180, see Fig. 8 for an alignment of the ectodomains of TSHr, LH/CGr, and FSHr). Bhowmick *et al.* (31) substituted R, Q, G, and E for K180 in LH/CGr (K158 in their numbering). Considering the loss of binding of hCG to the K180E mutant, they suggested that K180 in LH/CGr is important for binding of hCG. Our results suggest that, in the wt TSHr, this lysine being involved in a salt bridge with E157 would be neither attractive nor repulsive for hCG, whereas in K183 mutants, it could obvi-

	LRR1	LRR2	LRR3	LRR4	LRR5	LRR6	LRR7	LRR8	LRR9
TSHr									
X_1	Q55	S79	T104	K129	F154	L180	D203	S229	K250
X_2	T56	R80	H105	F130	I155	T181	A204	L230	E251
L									
X_3	K58	Y82	E107	G132	E157	K183	Y206	D232	I253
L									
X_4	I60	S84	R109	F134	T159	Y185	N208	S234	R255
X_5	E61	I85	N110	N135	D160	N186	K209	Q235	N256
LH/CGr									
X_1	T52	I76	S101	K126	F151	V177	T200	K225	Q246
X_2	R53	K77	E102	Y127	I152	T178	S201	T226	R247
L									
X_3	S55	E79	L104	S129	E154	K180	E203	D228	I249
L									
X_4	A57	S81	Q106	C131	C156	Y182	K205	S230	T251
X_5	Y58	Q82	N107	N132	D157	G183	E206	S231	S252
FSHr									
X_1	I49	E73	H98	Q123	V147	V173	D196	V221	K242
X_2	E50	K74	E99	Y124	L148	I174	E197	I222	K243
L									
X_3	R52	E76	R101	L126	D150	W176	N199	D224	R245
L									
X_4	V54	S78	E103	S128	Q152	N178	S201	S226	R247
X_5	L55	Q79	K104	N129	D153	K179	D202	R227	S248

Fig. 8. Alignment of the β-Strands of the Nine LRRs of the Ectodomains of TSHr, LH/CGr, and FSHr

A typical β-strand of a LRR is composed of eight amino acids: $LX_1X_2LX_3LX_4X_5$ (X, any amino acid; L, leucine, isoleucine, valine, or rarely, methionine or alanine; Ref. 24). According to the proposed structural models (24–26), the lateral chains of L amino acids are pointing inside the hydrophobic core of the protein, whereas those of the X residues are directed toward the surface the protein, and accordingly, are supposed to contact the ligands (24–26). In this alignment, only the X amino acids are represented to better visualize the inner cusp of the ectodomain that faces hormones and the possible interactions between side chains of these amino acids. The numbering starts from the first amino acid of the signal peptide of each receptor.

ously not play a role in the gain of function toward hCG. We can interpret this apparent discrepancy in two ways. First, the role of lysine 183 in TSHr and lysine 180 in LH/CGr must be critically dependent on their surrounding amino acids, which are significantly different in TSHr and LH/CGr (see Fig. 8), in particular when considering charged and polar residues. In the same spirit, the geometry of the interaction of hCG with the TSHr and LH/CGr may be different, implying that hCG could make contacts with different homologous residues in the ectodomains of the two receptors. It must also be noted that the conclusions of Bhowmick *et al.* about an important role of K180 for the binding of hCG in LH/CGr are drawn from loss-of-function mutants, while ours about the neutral role of K183 in the TSHr are drawn from gain-of-function mutants, which avoids the pitfalls related to misfolding and/or absence from cell surface.

An Acidic Residue in Positions Homologous to Residue 157 of TSHr Is Found in All the Glycoprotein Hormone Receptors

Our results show that, when the region surrounding amino acid positions 157 and 183 in TSHr is rendered more electronegative (as represented in Fig. 3 with mutants K183A and E157A+K183E), hCG seems to be specifically attracted. This suggests that hCG could harbor positively charged residues that would make specific interactions with the electronegative region of the mutant TSH receptors. The arginine residues in positions 94 and 95 of the seat-belt region of hCG β-subunit are good candidates, having been shown to be essential for LH/CGr activation (12, 30) and to give modest LH/CGr activation or binding capabilities to mutant TSH or FSH bearing these two residues (32, 33). This hypothesis could be easily tested by stimulation of our mutant receptors with the above-mentioned mutant hormones.

Intriguingly, all the glycoprotein hormone receptors [even a distant *Drosophila* homologue (34)] have an acidic residue in the position homologous to E157 in the TSHr. The functional or structural meaning of this observation is expected to be different whether the residue would be involved, or not, in a neutralizing interaction with a nearby basic residue. Although not amenable to direct experimental investigation, one hypothesis would be that an acidic residue was present in this position in the ancestral glycoprotein hormone receptor, and that it was implicated in recognition of the ancestral hormone. Although it was conserved in all, in some receptors, such as the LH/CGr, it would still play that role [in keeping with this view, an E132K mutant of LH/CGr displays decreased binding of hCG (26)], whereas in others, such as the TSHr, it would have been neutralized as part of the evolutionary mechanism leading to the specificity of recognition in the various hormone/receptor couples. In addition, and compatible with the above hypothesis, it is possible that an acidic residue in position homologous to 157 would be important for the precise structural integrity of the glycoprotein hormone receptors. The small increase in EC_{50} for TSH in E157A and most double mutants would be compatible with this view.

Additional Natural Mutations in Position 183 of TSHr Are Expected to be Found in Gestational Hyperthyroidism

It must be kept in mind that the gain of function of the K183 mutants toward hCG is modest. As noted in the original description for the K183R mutant, and confirmed in the present study for the other K183 substitutions, the affinity for hCG is too low to permit detection of specific I^{125}hCG binding to transfected COS cells. The EC_{50} of the best mutants for hCG is in the range of 10 mIU/ml, which is about 3 orders of magnitude higher than with wt LH/CGr (27). In view of the very high concentrations of hCG during the first trimester of pregnancy, this modest increase in responsiveness of K183R to hCG was, however, sufficient to cause severe hyperthyroidism (27). The present results indicate that other spontaneous mutations of K183 would be expected to produce a similar phenotype. Indeed, six of the mutations tested (K183R, N, Q, M, E, T) could result from a single nucleotide substitution in the K183 codon. This poses the question of why familial gestational hyperthyroidism remains presently limited to the description of a single family. Amongst plausible explanations one may cite: 1) a strong

negative selection due to the reduction in reproductive fitness of the women carrying the mutations; 2) the possibility that some of the mutants tested here in COS cells (*e.g.* K183E and K183T) would be expressed at too low a level in thyrocytes to cause significant stimulation of cAMP production. Note, however, that in COS cells, K183M, N, and Q mutants have the same capacity to stimulate cAMP production in response to hCG as K183R (see Fig. 2B); 3) the possibility that the situation would simply be underdiagnosed. Considering the steep increase in hCG during the first trimester of pregnancy, biological hyperthyroidism might develop too quickly to be diagnosed before miscarriage would occur. As fetal loss, with rapidly falling hCG, constitutes the "natural cure" of the condition, spontaneously resolving hyperthyroidism may remain undiagnosed in these patients. If this holds true, it might be valuable to search for this type of mutation amongst patients with recurrent spontaneous abortions.

In conclusion, our results point to lysine 183 and glutamic acid 157 in the ectodomain of TSHr as two important residues implicated in determining the specificity of recognition by TSH and hCG. Investigation of their role by a combination of site-directed mutagenesis experiments and molecular dynamic simulations, and the coherent emerging picture in the context of the available structural model of TSHr ectodomain, illustrates the promises of the approach. In the absence of crystallographic data of hormone-receptor complexes, a similar strategy should now be used to tackle in a more global way the problem of the evolution of specificity in all three glycoprotein hormone receptors.

MATERIALS AND METHODS

Reagents

Plasmid pBluescript SK$^+$ was obtained from Stratagene (La Jolla, CA); plasmid pSVL was obtained from Amersham Pharmacia Biotech (Roosendaal, The Netherlands). Restriction enzymes were obtained from Life Technologies, Inc. (Merelbeke, Belgium) and New England Biolabs, Inc. (Beverly, MA). *Pfu* Turbo polymerase was obtained from Stratagene. Monoclonal antibody 3G4 was obtained by genetic immunization with the cDNA coding for the human TSHr as already described (18) and was directed against a linear epitope (residues 354–360, VFFEEQE) on the TSHr ectodomain.

Construction of the TSHr Mutants

Mutations (K183R, A, I, T, E, W, D, M, N, or Q; E157A; E157D) were introduced in the hTSHr by QuikChange (Stratagene) site-directed mutagenesis method, starting with hTSHr in pBluescript SK$^+$, as previously described (35, 36). The primers are available upon request. The appropriate mutated portions of hTSHr mutants were subcloned in pSVL-hTSHr cDNA with *Xho*I and *Afl*III to obtain the 12 mutants expected.

Mutants E157A+K183R, A, I, T, E, W, D, M, N, or Q and E157D+K183R, A, or W were constructed by subcloning: mutations in position 157 were excised from pBluescript SK$^+$-E157A or D-hTSHr by *Xho*I–*Aat*II; mutations in position 183 were excised from pBluescript SK$^+$-K183R, A, I, T, E, W, D, M, N, or Q-hTSHr by *Aat*II–*Afl*III. Fragments bearing one E157 mutation and one K183 mutation were ligated in pSVL-hTSHr which had been cleaved by *Xho*I–*Afl*III to obtain the 13 mutants expected.

All the constructs were amplified in DH5αF′-competent cells, and recombinant DNA from selected clones was purified and sequenced for confirmation of the nucleotide sequences of the PCR-generated areas.

Transfection Experiments

COS-7 cells were used for transient expression allowing functional assays. They were transfected by the diethylaminoethyl-dextran method followed by a dimethylsulfoxide shock as described previously (37, 38). Two days after transfection, cells were used for cAMP determinations and flow immunocytofluorometry. Duplicate or triplicate dishes were used for each assay. Each experiment was repeated at least twice. Cells transfected with pSVL alone were always run as controls.

Quantification of Cell Surface Expression of TSHr Constructs by Fluorescence Activated Cell Sorter

Cells were prepared as previously described (18). After detachment, they were centrifuged at 500 $\times$ *g* at 4 C for 3 min and the supernatant was removed by inversion. They were incubated for 30 min at room temperature with 100 μl PBS-BSA 0.1% containing the 3G4 monoclonal antibody obtained from genetic immunization with the wt hTSHr cDNA (18). Cells were then washed with 4 ml PBS-BSA 0.1% and centrifuged as above. They were incubated on ice in the dark with fluorescein-conjugated γ-chain-specific goat antimouse IgG (Sigma, St. Louis, MO) in the same buffer. Propidium iodide (10 μg/ml) was used for detection of damaged cells that were excluded from the analysis. Cells were washed and resuspended in 300 μl PBS-BSA 0.1%. The fluorescence of 10,000 cells/tube was assayed by a FACScan flow cytofluorometer (Becton Dickinson and Co., Eerenbodegem, Belgium). Cells transfected by pSVL alone and by pSVL-hTSHr wt cDNA were always run as negative and positive controls, respectively.

Determination of cAMP Production

For cAMP determinations, culture medium was removed 48 h after transfection and replaced by Krebs-Ringer-HEPES buffer for 30 min. Thereafter, cells were incubated for 60 min in fresh Krebs-Ringer-HEPES buffer supplemented with 25 μM of the phosphodiesterase inhibitor Rolipram (Laboratoire Logeais, Paris, France) and various concentrations of highly purified hCG (Sigma), bovine TSH (Sigma), or recombinant FSH (Organon Belge SA, Brussels, Belgium). At the end of a 1-h incubation, the medium was discarded and replaced with 0.1 M HCl. The cell extracts were dried in a vacuum concentrator, resuspended in water, and diluted appropriately for cAMP measurements by RIA according to the method of Brooker *et al.* (39). Duplicate samples were assayed in all experiments; results are expressed in picomoles cAMP per milliliter. Concentration-action curves were fitted with the Prism computer program (GraphPad Software, Inc., San Diego, CA).

Molecular Modeling and Molecular Dynamics Simulations of the Extracellular Domain of the TSHr

The atomic coordinates of the extracellular domain of the TSHr (24), constructed from the structure of the porcine ribonuclease inhibitor (23), were employed in the simulations. Molecular models for the mutant receptors containing the single K183A substitution and the double E157A+K183E substitutions were built from these coordinates by amino acid replacement, whereas the K183R mutant receptor was built from an exhaustive surveyed of all permitted Arg side-chain conformations. These permitted conformations of the χ_1, χ_2, χ_3, and χ_4 torsional angles were taken from a backbone-dependent rotamer library (28), from which we selected the

rotamers corresponding to the backbone conformation of residue 183 of the model ($\phi = -90°$ and $\psi = 130°$). Only conformations that are described to occur at least 1% of the time in the known crystal structures were considered. This leads to 27 rotamers of the 81 theoretically possible rotamers. To identify potential ionic partners of R183, we calculated the distances between the N_ϵ, N_{H1}, and N_{H2} atoms of R183 and the $O_{\epsilon 1}$ and $O_{\epsilon 2}$ or $O_{\delta 1}$ and $O_{\delta 2}$ atoms of Asp and Glu residues, for all the considered conformations of the Arg side chain. To assess which rotamers were favorable for ionic interaction, we retained conformers leading to minimal N↔O distance in the 2.0–4.0 Å range. The resulting structures were placed in a rectangular box containing Monte Carlo-equilibrated TIP3P water molecules. The periodic boxes were approximately 75 Å × 50 Å × 50 Å, and contained between 4059 and 4348 water molecules in addition to the extracellular domain. Initially, the atoms of the receptor were kept fixed, whereas the water molecules were energy minimized (500 steps). Subsequently, the entire systems were energy minimized (500 steps), heated [from 0 to 300 K in 15 picoseconds (ps)], equilibrated (from 15 to 200 ps), and the production run (from 200 to 500 ps) was carried out at constant pressure using the particle mesh Ewald method to evaluate electrostatic interactions (40). Structures were collected every 5 ps during the last 300 ps of simulation (60 structures per simulation). The molecular dynamics simulations were run with the Sander module of AMBER 5 (41, 41a; and http://www.amber.ucsf.edu/amber), the all-atom force field (42), SHAKE bond constraints in all bonds (42a), a 2-femtosecond integration time step, and constant temperature of 300 K coupled to a heat bath. The molecular electrostatic potentials on the accessible surface of representative structures were calculated and displayed with GRASP (43; and http://trantor.bioc.columbia.edu/grasp) using the Cornell *et al.* (42) atomic charges. The interactions of R183 in the K183R mutant receptor with D232 and its neighbor residues were further characterized by *ab initio* quantum mechanical calculations. We performed full geometry optimization at the MP2/6–31G* level of theory, which is capable of describing the proposed N-H··π interactions (44) in a model system containing the following molecular fragments: the side chains of R183 (the -C_β-C_γ-C_δ- chain was replaced by a hydrogen), Y185 and Y206 (the -C_β- and –OH moieties were replaced by hydrogens), and N208 and D232 (the -C_β- moieties were replaced by a hydrogen). All the quantum mechanical calculations were performed with the Gaussian 98 (Revision A.7) system of programs (45; and http://www.gaussian.com).

Acknowledgments

We thank S. Wodack for critical advice and C. Massart for technical assistance.

Received August 10, 2001. Accepted December 21, 2001.

Address all correspondence and requests for reprints to: Gilbert Vassart, Institut de Recherche Interdisciplinaire en Biologie Humaine et Nucléaire, Université Libre de Bruxelles, Campus Erasme, 808 route de Lennik, B-1070 Bruxelles, Belgium. E-mail: gvassart@ulb.ac.be.

G.S. was supported by Horlait-Dapsens funding. S.C. is Research Associate at the Belgian Fonds National de la Recherche Scientifique. This study was supported by the Belgian State, Prime Minister's office, Service for Sciences, Technology, and Culture. This work was also supported by grants from the Fonds de la Recherche Scientifique Médicale, Fonds National de la Recherche Scientifique, Association Recherche Biomédicale et Diagnostic, and BRAHMS Diagnostics, and in part by grants from Comision Interministerial de Ciencia y Tecnologia (SAF99-073), Fundació La Marató TV3 (0014/97), the Improving Human Potential of the European Community (HPRI-CT-1999-00071), and the MINOS (Multidisciplinary Intensive Computing for Research Activities of European Scientists) Project. Computer facilities were provided by the Centre de Computació i Comunicacions de Catalunya.

REFERENCES

1. Libert F, Lefort A, Gerard C, Parmentier M, Perret J, Ludgate M, Dumont JE, Vassart G 1989 Cloning, sequencing and expression of the human thyrotropin (TSH) receptor: evidence for binding of autoantibodies. Biochem Biophys Res Commun 165:1250–1255
2. Nagayama Y, Kaufman KD, Seto P, Rapoport B 1989 Molecular cloning, sequence and functional expression of the cDNA for the human thyrotropin receptor. Biochem Biophys Res Commun 165:1184–1190
3. McFarland KC, Sprengel R, Phillips HS, Kohler M, Rosemblit N, Nikolics K, Segaloff DL, Seeburg PH 1989 Lutropin-choriogonadotropin receptor: an unusual member of the G protein-coupled receptor family. Science 245:494–499
4. Loosfelt H, Misrahi M, Atger M, Salesse R, Vu Hai Luu Thi MT, Jolivet A, Guiochon Mantel A, Sar S, Jallal B, Garnier J, Milgrom E 1989 Cloning and sequencing of porcine LH-hCG receptor cDNA: variants lacking transmembrane domain. Science 245:525–528
5. Minegishi T, Nakamura K, Takakura Y, Miyamoto K, Hasegawa Y, Ibuki Y, Igarashi M, Minegish T 1990 Cloning and sequencing of human LH/hCG receptor cDNA [published erratum appears in Biochem Biophys Res Commun 1994 Jun 15;201(2):1057]. Biochem Biophys Res Commun 172:1049–1054
6. Minegishi T, Nakamura K, Takakura Y, Ibuki Y, Igarashi M, Minegish T 1991 Cloning and sequencing of human FSH receptor cDNA. Biochem Biophys Res Commun 175:1125–1130
7. Lapthorn AJ, Harris DC, Littlejohn A, Lustbader JW, Canfield RE, Machin KJ, Morgan FJ, Isaacs NW 1994 Crystal structure of human chorionic gonadotropin. Nature 369:455–461
8. Fox KM, Dias JA, Van Roey P 2001 Three-dimensional structure of human follicle-stimulating hormone. Mol Endocrinol 15:378–389
9. Rapoport B, Chazenbalk GD, Jaume JC, McLachlan SM 1998 The thyrotropin (TSH) receptor: interaction with TSH and autoantibodies. Endocr Rev 19:673–716
10. Themmen APN, Huhtaniemi IT 2000 Mutations of gonadotropins and gonadotropin receptors: elucidating the physiology and pathophysiology of pituitary-gonadal function. Endocr Rev 21:551–583
11. Boime I, Ben Menahem D 1999 Glycoprotein hormone structure-function and analog design. Recent Prog Horm Res 54:271–288
12. Moyle WR, Campbell RK, Myers RV, Bernard MP, Han Y, Wang X 1994 Co-evolution of ligand-receptor pairs. Nature 368:251–255
13. Braun T, Schofield PR, Sprengel R 1991 Amino-terminal leucine-rich repeats in gonadotropin receptors determine hormone selectivity. EMBO J 10:1885–1890
14. Remy JJ, Nespoulous C, Grosclaude J, Grebert D, Couture L, Pajot E, Salesse R 2001 Purification and structural analysis of a soluble human chorionogonadotropin hormone-receptor complex. J Biol Chem 276:1681–1687
15. Schmidt A, MacColl R, Lindau-Shepard B, Buckler DR, Dias JA 2001 Hormone-induced conformational change of the purified soluble hormone binding domain of follitropin receptor complexed with single chain follitropin. J Biol Chem 276:23373–23381
16. Osuga Y, Liang SG, Dallas JS, Wang C, Hsueh AJ 1998 Soluble ecto-domain mutant of thyrotropin (TSH) receptor incapable of binding TSH neutralizes the action of thyroid-stimulating antibodies from Graves' patients. Endocrinology 139:671–676

17. Da Costa CR, Johnstone AP 1998 Production of the thyrotrophin receptor extracellular domain as a glycosylphosphatidylinositol-anchored membrane protein and its interaction with thyrotrophin and autoantibodies. J Biol Chem 273:11874–11880
18. Costagliola S, Khoo D, Vassart G 1998 Production of bioactive amino-terminal domain of the thyrotropin receptor via insertion in the plasma membrane by a glycosylphosphatidylinositol anchor. FEBS Lett 436:427–433
19. Gether U 2000 Uncovering molecular mechanisms involved in activation of G protein-coupled receptors. Endocr Rev 21:90–113
20. Morris AJ, Malbon CC 1999 Physiological regulation of G protein-linked signaling. Physiol Rev 79:1373–1430
21. Palczewski K, Kumasaka T, Hori T, Behnke CA, Motoshima H, Fox BA, Le Trong, I, Teller DC, Okada T, Stenkamp RE, Yamamoto M, Miyano M 2000 Crystal structure of rhodopsin: a G protein-coupled receptor. Science 289:739–745
22. Kobe B, Deisenhofer J 1995 A structural basis of the interactions between leucine-rich repeats and protein ligands. Nature 374:183–186
23. Kobe B, Deisenhofer J 1993 Crystal structure of porcine ribonuclease inhibitor, a protein with leucine-rich repeats. Nature 366:751–756
24. Kajava AV, Vassart G, Wodak SJ 1995 Modeling of the three-dimensional structure of proteins with the typical leucine-rich repeats. Structure 3:867–877
25. Jiang X, Dreano M, Buckler DR, Cheng S, Ythier A, Wu H, Hendrickson WA, el Tayar N 1995 Structural predictions for the ligand-binding region of glycoprotein hormone receptors and the nature of hormone-receptor interactions. Structure 3:1341–1353
26. Bhowmick N, Huang J, Puett D, Isaacs NW, Lapthorn AJ 1996 Determination of residues important in hormone binding to the extracellular domain of the luteinizing hormone/chorionic gonadotropin receptor by site-directed mutagenesis and modeling. Mol Endocrinol 10:1147–1159
27. Rodien P, Bremont C, Sanson ML, Parma J, Van Sande J, Costagliola S, Luton JP, Vassart G, Duprez L 1998 Familial gestational hyperthyroidism caused by a mutant thyrotropin receptor hypersensitive to human chorionic gonadotropin. N Engl J Med 339:1823–1826
28. Dunbrack Jr RL, Cohen FE 1997 Bayesian statistical analysis of protein side-chain rotamer preferences. Protein Sci 6:1661–1681
29. Steiner T, Koellner G 2001 Hydrogen bonds with pi-acceptors in proteins: frequencies and role in stabilizing local 3D structures. J Mol Biol 305:535–557
30. Campbell RK, Bergert ER, Wang Y, Morris JC, Moyle WR 1997 Chimeric proteins can exceed the sum of their parts: implications for evolution and protein design. Nat Biotechnol 15:439–443
31. Bhowmick N, Narayan P, Puett D 1999 Identification of ionizable amino acid residues on the extracellular domain of the lutropin receptor involved in ligand binding. Endocrinology 140:4558–4563
32. Dias JA, Zhang Y, Liu X 1994 Receptor binding and functional properties of chimeric human follitropin prepared by an exchange between a small hydrophilic intercysteine loop of human follitropin and human lutropin. J Biol Chem 269:25289–25294
33. Grossmann M, Szkudlinski MW, Wong R, Dias JA, Ji TH, Weintraub BD 1997 Substitution of the seat-belt region of the thyroid-stimulating hormone (TSH) β-subunit with the corresponding regions of choriogonadotropin or follitropin confers luteotropic but not follitropic activity to chimeric TSH. J Biol Chem 272:15532–15540
34. Hauser F, Nothacker HP, Grimmelikhuijzen CJ 1997 Molecular cloning, genomic organization, and developmental regulation of a novel receptor from Drosophila melanogaster structurally related to members of the thyroid-stimulating hormone, follicle-stimulating hormone, luteinizing hormone/choriogonadotropin receptor family from mammals. J Biol Chem 272:1002–1010
35. Ansaldi M, Lepelletier M, Mejean V 1996 Site-specific mutagenesis by using an accurate recombinant polymerase chain reaction method. Anal Biochem 234:110–111
36. Ho SC, Van Sande J, Lefort A, Vassart G, Costagliola S 2001 Effects of mutations involving the highly conserved S281HCC motif in the extracellular domain of the thyrotropin (TSH) receptor on TSH binding and constitutive activity. Endocrinology 142:2760–2767
37. Lopata MA, Cleveland DW, Sollner-Webb B 1984 High level transient expression of a chloramphenicol acetyl transferase gene by DEAE-dextran mediated DNA transfection coupled with a dimethyl sulfoxide or glycerol shock treatment. Nucleic Acids Res 12:5707–5717
38. Govaerts C, Lefort A, Costagliola S, Wodak SJ, Ballesteros JA, Van Sande J, Pardo L, Vassart G 2001 A conserved ASN in TM7 is a on/off switch in the activation of the TSH receptor. J Biol Chem 276:22991–22999
39. Brooker G, Harper JF, Terasaki WL, Moylan RD 1979 Radioimmunoassy of cyclic AMP and cyclic GMP. Adv Cyclic Nucl Res 10:1–33
40. Darden T, York D, Pedersen L 1993 Particle mesh Ewald: an N·log(N) method for Ewald sums in large systems. J Chem Phys 98:10089–10092
41. Case DA, Pearlman DA, Caldwell JW, Cheatham TE, Ross WS, Simmerling CL, Darden TA, Merz KM, Stanton RV, Cheng AL, Vincent J, Crowley M, Ferguson DM, Radmer RJ, Seibel GL, Singh UC, Weiner PK, Kollman PA 1997 AMBER 5, University of California, San Francisco

41a. Pearlman DA, Case DA, Caldwell JW, Ross WS, Cheatham TE, DeBolt S, Ferguson DM, Seibel GL, Kollman PA 1995 AMBER, a package of computer programs for applying molecular mechanics, normal mode analysis, molecular dynamics and free energy calculations to simulate the structural and energetic properties of molecules. Comput Phys Commun 91:1–41

42. Cornell WD 1995 A second generation force field for the simulation of proteins, nucleic acids, and organic molecules. J Am Chem Soc 117:5179–5197

42a. Ryckaert JP, Ciccotti G, Berendsen HJC 1977 Numerical integration of the cartesian equation of motion of a system with constraints: molecular dynamics of n-alkanes. J Comput Phys 23:327–341

43. Nicholls A, Sharp KA, Honig B 1991 Protein folding and association: insights from the interfacial and thermodynamic properties of hydrocarbons. Proteins 11:281–296
44. Tsuzuki S, Honda K, Uchimaru T, Mikami M, Tanabe K 2000 Origin of the attraction and directionality of the NH/π interaction: comparison with OH/π and CH/π interactions. J Am Chem Soc 122:11450–11458
45. Frisch MJ, Trucks GW, Schlegel HB, Scuseria GE, Robb MA, Cheeseman JR, Zakrzewski VG, Montgomery JA, Keith TA, Petersson GA, Raghavachari K, Al Laham A, Stratmann RE, Burant JC, Dapprich S, Millam JM, Daniels AD, Kudin KN, Strain MC, Farkas O, Tomasi J, Barone V, Cossi M, Cammi R, Mennucci B, Pomelli C, Adamo C, Clifford S, Ochterski J, Petersson GA, Ayala PY, Cui Q, Morokuma K, Malick DK, Rabuck AD, Raghavachari K, Foresman JB, Cioslowski J, Ortiz JV, Stefanov BB, Liu G, Liashenko A, Piskorz P, Komaromi I, Gomperts R, Martin RL, Fox DJ, Keith T, Al Laham MA, Peng CY, Nanayakkara A, Gonzalez C, Challacombe M, Gill PMW, Johnson BG, Chen W, Wong W, Andres JL, Head-Gordon M, Replogle ES, Pople JA 1998 Gaussian 98 (Revision A.7), Gaussian, Inc., Pittsburgh, PA